Full Paper Transactions, SMiRT 28
Toronto, Canada, August 10-15, 2025

A NUMERICALLY STABLE INTEGRATED SIMULATION METHOD WITH DIFFERENT TIME STEPS FOR SOIL-STRUCTURE INTERACTION ANALYSIS OF NUCLEAR STRUCTURES

Shangzhang Wang[1], Oh-Sung Kwon[2], Xu Huang[3]

[1] PhD Candidate, Wuhan University of Technology, Wuhan, China (shang_zhang@whut.edu.cn)
[2] Professor, University of Toronto, Toronto, Canada (os.kwon@utoronto.ca)
[3] Research Associate, University of Toronto, Toronto, Canada (xu.huang87@gmail.com)

ABSTRACT

Compared with monolithic simulation methods, integrated simulation methods allow for the decomposition of large complex systems into several subsystems, and the behavior of these subsystems can be numerically captured using independent analysis tools. To ease implementation and ensure numerical stability, a numerically stable integrated simulation method, termed the WHK method, was previously proposed. In this study, the WHK method is further generalized with different time steps (WHK-DTS) for the decomposed subsystems. The method is characterized by the following features: (1) it allows for multiplatform simulation with different numerical integrators; (2) unconditionally stable solutions can be achieved, and the stability is independent of the time step ratios between the decomposed subsystems; and (3) the time step ratios are beneficial for expanding the stability boundary of subsystems when using conditionally stable integration schemes. The accuracy and numerical stability of the proposed method are verified through the soil-structure interaction (SSI) analysis of a Candu 6 nuclear containment building. By comparing with the standalone model of the entire SSI system, the integrated model using the proposed method shows good accuracy and higher computational efficiency, which demonstrates its potential for future SSI analysis of nuclear structures.

INTRODUCTION

Compared with monolithic simulation methods, integrated simulation methods allow for decomposing a complex or large-scale dynamic system into multiple subsystems, which can be solved with different integration schemes. Among various integrated simulation methods, the HK method, developed by Huang et al (2020), extends the implementation from a single finite element (FE) simulation platform to multiple platforms with good accuracy and acceptable numerical stability. The HK method enables each decomposed subsystem to be modeled independently using an appropriate FE software package. Furthermore, the WHK method developed by Wang et al. (2024) expands the application of the multiplatform integrated simulation method by improving the numerical stability. Unconditionally stable solutions can be achieved through the proper selection of numerical integration schemes and their coefficients. This avoids using a small time step for the HK method, which could compromise the usual advantage of integrated simulation methods in enhancing computational efficiency (Huang et al. 2024). Although the above-integrated simulation methods allow different subsystems to have their time integrators, it limits them to have the same time step size. In fact, in SSI analysis, soil, and structure have significantly different response characteristics, and the subsystems need to adjust the time step according to their specificity (Chen et al. 2022). Therefore, it is imperative to develop different time-step methods (DTS).

In this study, the WHK method has been generalized to an integrated simulation method with different time steps, which is called the WHK-DTS method. Compared with existing DTS methods, the proposed method has the following features: (1) Based on the WHK method, the proposed method allows for multiple partitioned simulations with different numerical integrators. (2) Unconditionally stable solutions can be

achieved and the stability is independent of the time step ratios between the decomposed subsystems. (3) The time step ratios are beneficial for expanding the stability boundary of subsystems when using conditionally stable integration schemes.

The structure of this paper is organized as Section 2 introduces the WHK-DTS method and presents its data exchange strategy. Section 3 provides an SSI application to demonstrate the method's feasibility and applicability in finite element tools, along with its computational efficiency advantages. Finally, Section 4 summarizes the results and findings.

PROPOSED METHOD

The proposed WHK-DTS method is introduced in this section through a four-degree-of-freedom (DOF) dynamic system, as shown in Figure 1. The system is divided into three subsystems: Sub-*i*, Sub-*j*, and Sub-*k*, and they are solved using different Newmark-β integration schemes with different time steps. It is assumed that Sub-*i* uses a time step δt which is smaller than the time step Δt used for both Sub-*j* and Sub-*k*. Then the time step ratio m is $\Delta t/\delta t$. After discretization of the time and space domains, the EOM of Sub-*i* can be written as

$$\boldsymbol{M}_i\ddot{\boldsymbol{x}}_{i,n+\frac{s}{m}} + \boldsymbol{C}_i\dot{\boldsymbol{x}}_{i,n+\frac{s}{m}} + \boldsymbol{K}_i\boldsymbol{x}_{i,n+\frac{s}{m}} = \boldsymbol{F}_{i,n+\frac{s}{m}} + \boldsymbol{P}_{ij,n+\frac{s}{m}} \tag{1}$$

where the subscripts *i* and *j* denote the terms associated with Sub-*i* and Sub-*j*, respectively. The subscripts *n* and *s* are integers and $n+\frac{s}{m}$ represents the time step of $n\times\Delta t + s\times\delta t$, where $m \geq s \geq 1$. $\boldsymbol{M}$, $\boldsymbol{C}$, and $\boldsymbol{K}$ are the mass, damping, and stiffness matrices. $\boldsymbol{x}$, $\dot{\boldsymbol{x}}$ and $\ddot{\boldsymbol{x}}$ are the displacement, velocity, and acceleration vectors, respectively; $\boldsymbol{F}$ is the external load vector. The term $\boldsymbol{P}_{ij}$ represents the interaction force imposed by Sub-*j* on Sub-*i*. The details of the terms in Eq. (1) are expressed below:

$$\boldsymbol{M}_i = \begin{bmatrix} \boldsymbol{m}_i^{II} & \boldsymbol{m}_i^{IB_i} \\ \boldsymbol{m}_i^{B_iI} & \boldsymbol{m}_i^{B_iB_i} \end{bmatrix}, \boldsymbol{C}_i = \begin{bmatrix} \boldsymbol{c}_i^{II} & \boldsymbol{c}_i^{IB_i} \\ \boldsymbol{c}_i^{B_iI} & \boldsymbol{c}_i^{B_iB_i} \end{bmatrix}, \boldsymbol{K}_i = \begin{bmatrix} \boldsymbol{k}_i^{II} & \boldsymbol{k}_i^{IB_i} \\ \boldsymbol{k}_i^{B_iI} & \boldsymbol{k}_i^{B_iB_i} \end{bmatrix} \tag{2}$$

$$\boldsymbol{F}_{i,n+\frac{s}{m}} = \begin{bmatrix} \boldsymbol{f}_{i,n+\frac{s}{m}}^{I} \\ \boldsymbol{f}_{i,n+\frac{s}{m}}^{B_i} \end{bmatrix}, \boldsymbol{x}_{i,n+\frac{s}{m}} = \begin{bmatrix} \boldsymbol{x}_{i,n+\frac{s}{m}}^{I} \\ \boldsymbol{x}_{i,n+\frac{s}{m}}^{B_i} \end{bmatrix} \tag{3}$$

$$\boldsymbol{P}_{ij,n+\frac{s}{m}} = \begin{bmatrix} \boldsymbol{0} \\ -\left(\boldsymbol{m}_j^{B_iB_i}\ddot{\boldsymbol{x}}_{j,n+\frac{s}{m}}^{B_i} + \boldsymbol{c}_j^{B_iB_i}\dot{\boldsymbol{x}}_{j,n+\frac{s}{m}}^{B_i} + \boldsymbol{k}_j^{B_iB_i}\boldsymbol{x}_{j,n+\frac{s}{m}}^{B_i} + \boldsymbol{c}_j^{B_iB_k}\dot{\boldsymbol{x}}_{j,n+\frac{s}{m}}^{B_k} + \boldsymbol{k}_j^{B_iB_k}\boldsymbol{x}_{j,n+\frac{s}{m}}^{B_k}\right) \end{bmatrix} \tag{4}$$

where the superscript *I* indicates the terms associated with the internal DOFs of the subsystems, and B_i and B_k denote the terms associated with the DOFs at the interface boundaries of B_i and B_k, respectively.

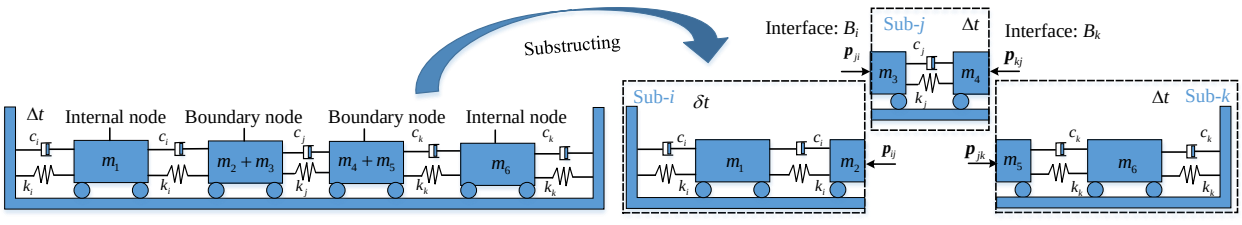

Figure 1. Four-DOF dynamic system

For Sub-*i*, the displacement and velocity expressions of the Newmark-β integration scheme are

$$\boldsymbol{x}_{i,n+\frac{s}{m}} = \widetilde{\boldsymbol{x}}_{i,n+\frac{s}{m}} + \beta_{i,2}\delta t^2 \ddot{\boldsymbol{x}}_{i,n+\frac{s}{m}}, \quad \dot{\boldsymbol{x}}_{i,n+\frac{s}{m}} = \widetilde{\dot{\boldsymbol{x}}}_{i,n+\frac{s}{m}} + \gamma_{i,2}\delta t \ddot{\boldsymbol{x}}_{i,n+\frac{s}{m}} \tag{5}$$

where β and γ are the coefficients of the Newmark-β integration scheme. $\widetilde{\boldsymbol{x}}$ and $\widetilde{\dot{\boldsymbol{x}}}$ are the predicted displacement and velocity, respectively, which can be expressed as

$$\widetilde{\boldsymbol{x}}_{i,n+\frac{s}{m}} = \boldsymbol{x}_{i,n+\frac{s-1}{m}} + \delta t \dot{\boldsymbol{x}}_{i,n+\frac{s-1}{m}} + \beta_{i,1}\delta t^2 \ddot{\boldsymbol{x}}_{i,n+\frac{s-1}{m}}, \quad \widetilde{\dot{\boldsymbol{x}}}_{i,n+\frac{s}{m}} = \dot{\boldsymbol{x}}_{i,n+\frac{s-1}{m}} + \gamma_{i,1}\delta t \ddot{\boldsymbol{x}}_{i,n+\frac{s-1}{m}} \tag{6}$$

The terms associated with the interface boundary B_i of Sub-*j* in Eq. (4) are expressed by the Newmark-β integration scheme, which is

$$\boldsymbol{x}_{j,n+1}^{B_i} = \widetilde{\boldsymbol{x}}_{j,n+1}^{B_i} + \beta_{j,2}\Delta t^2 \ddot{\boldsymbol{x}}_{j,n+1}^{B_i}, \quad \dot{\boldsymbol{x}}_{j,n+1}^{B_i} = \widetilde{\dot{\boldsymbol{x}}}_{j,n+1}^{B_i} + \gamma_{j,2}\Delta t \ddot{\boldsymbol{x}}_{j,n+1}^{B_i} \tag{7}$$

To solve Eq. (1) for Sub-*i*, the following assumptions are made:

- To ensure the compatibility of the boundary B_i, the accelerations are identical, which is

$$\ddot{\boldsymbol{x}}_{i,n+\frac{s}{m}}^{B_i} = \ddot{\boldsymbol{x}}_{j,n+\frac{s}{m}}^{B_i} = \ddot{\boldsymbol{x}}_{n+\frac{s}{m}}^{B_i} \tag{8}$$

- The state variables associated with boundary B_k in Eq. (4) are replaced with their predicted values, that is

$$\boldsymbol{c}_j^{B_iB_k}\dot{\boldsymbol{x}}_{j,n+\frac{s}{m}}^{B_k} + \boldsymbol{k}_j^{B_iB_k}\boldsymbol{x}_{j,n+\frac{s}{m}}^{B_k} \approx \boldsymbol{c}_j^{B_iB_k}\widetilde{\dot{\boldsymbol{x}}}_{j,n+\frac{s}{m}}^{B_k} + \boldsymbol{k}_j^{B_iB_k}\widetilde{\boldsymbol{x}}_{j,n+\frac{s}{m}}^{B_k} \tag{9}$$

- The predicted responses, i.e., $\widetilde{\boldsymbol{x}}$, or $\widetilde{\dot{\boldsymbol{x}}}$, follow the interpolation scheme as below

$$*_{j,n+\frac{s}{m}} = \left(1 - \frac{s}{m}\right) *_{j,n} + \frac{s}{m} *_{j,n+1} \tag{10}$$

where $*$ represents the predicted state variables of Sub-*j*,

By substituting Eqs. (5), (7), (8), (9) and (10) into Eq. (1), the EOM of Sub-*i* can be rewritten as

$$\left(\boldsymbol{A}_i + \boldsymbol{A}_{ij}\right)\ddot{\boldsymbol{x}}_{i,n+\frac{s}{m}} = \boldsymbol{B}_{i,n+\frac{s}{m}} + \boldsymbol{D}_{ij,n+\frac{s}{m}} \tag{11}$$

where

$$\boldsymbol{A}_i = \boldsymbol{M}_i + \gamma_{i,2}\delta t\boldsymbol{C}_i + \beta_{i,2}\delta t^2\boldsymbol{K}_i \tag{12}$$

$$\boldsymbol{B}_{i,n+\frac{s}{m}} = \boldsymbol{F}_{i,n+\frac{s}{m}} - \boldsymbol{C}_i\widetilde{\dot{\boldsymbol{x}}}_{i,n+\frac{s}{m}} - \boldsymbol{K}_i\widetilde{\boldsymbol{x}}_{i,n+\frac{s}{m}} \tag{13}$$

$$\boldsymbol{A}_{ij} = \boldsymbol{M}_j^{B_iB_i} + \gamma_{j,2}\Delta t\boldsymbol{C}_j^{B_iB_i} + \beta_{j,2}\Delta t^2\boldsymbol{K}_j^{B_iB_i} \tag{14}$$

$$\boldsymbol{D}_{ij,n+\frac{s}{m}} = \begin{bmatrix} \mathbf{0} \\ -\left(\boldsymbol{c}_j^{B_iB_i}\widetilde{\dot{\boldsymbol{x}}}_{j,n+\frac{s}{m}}^{B_i} + \boldsymbol{k}_j^{B_iB_i}\widetilde{\boldsymbol{x}}_{j,n+\frac{s}{m}}^{B_i} + \boldsymbol{c}_j^{B_iB_k}\widetilde{\dot{\boldsymbol{x}}}_{j,n+\frac{s}{m}}^{B_k} + \boldsymbol{k}_j^{B_iB_k}\widetilde{\boldsymbol{x}}_{j,n+\frac{s}{m}}^{B_k}\right) \end{bmatrix} \tag{15}$$

where $\boldsymbol{M}_j^{B_iB_i} = \begin{bmatrix} \mathbf{0} & \mathbf{0} \\ \mathbf{0} & \boldsymbol{m}_j^{B_iB_i} \end{bmatrix}$, $\boldsymbol{C}_j^{B_iB_i} = \begin{bmatrix} \mathbf{0} & \mathbf{0} \\ \mathbf{0} & \boldsymbol{c}_j^{B_iB_i} \end{bmatrix}$, and $\boldsymbol{K}_j^{B_iB_i} = \begin{bmatrix} \mathbf{0} & \mathbf{0} \\ \mathbf{0} & \boldsymbol{k}_j^{B_iB_i} \end{bmatrix}$

To make use of the updated acceleration data at each sub-time step, i.e., $\ddot{\boldsymbol{x}}_{n+\frac{s-1}{m}}^{B_i}$, the displacement and velocity predictions of the boundary B_i in Eq. (15) can be updated accordingly as

$$\begin{cases} \widetilde{\boldsymbol{x}}_{j,n+\frac{s}{m}}^{B_i} = \boldsymbol{x}_{j,n+\frac{s-1}{m}}^{B_i} + \delta t\dot{\boldsymbol{x}}_{j,n+\frac{s-1}{m}}^{B_i} + \beta_{j,1}\delta t^2\ddot{\boldsymbol{x}}_{n+\frac{s-1}{m}}^{B_i} \\ \widetilde{\dot{\boldsymbol{x}}}_{j,n+\frac{s}{m}}^{B_i} = \dot{\boldsymbol{x}}_{j,n+\frac{s-1}{m}}^{B_i} + \gamma_{j,1}\delta t\ddot{\boldsymbol{x}}_{n+\frac{s-1}{m}}^{B_i} \end{cases} \tag{16}$$

with

$$\begin{cases} \boldsymbol{x}_{j,n+\frac{s-1}{m}}^{B_i} = \widetilde{\boldsymbol{x}}_{j,n+\frac{s-1}{m}}^{B_i} + \beta_{j,2}\delta t^2\ddot{\boldsymbol{x}}_{j,n+\frac{s-1}{m}}^{B_i} \\ \dot{\boldsymbol{x}}_{j,n+\frac{s-1}{m}}^{B_i} = \widetilde{\dot{\boldsymbol{x}}}_{j,n+\frac{s-1}{m}}^{B_i} + \gamma_{j,2}\delta t\ddot{\boldsymbol{x}}_{j,n+\frac{s-1}{m}}^{B_i} \end{cases} \tag{17}$$

Since the state variables at the boundary B_k are computed using the large time step Δt, the predicted terms associated with the boundary B_k in Eq. (15) can be expressed as

$$\widetilde{\boldsymbol{x}}_{j,n+1}^{B_k} = \boldsymbol{x}_{j,n}^{B_k} + \Delta t\dot{\boldsymbol{x}}_{j,n}^{B_k} + \beta_{j,1}\Delta t^2\ddot{\boldsymbol{x}}_n^{B_k}, \quad \widetilde{\dot{\boldsymbol{x}}}_{j,n+1}^{B_k} = \dot{\boldsymbol{x}}_{j,n}^{B_k} + \gamma_{j,1}\Delta t\ddot{\boldsymbol{x}}_n^{B_k} \tag{18}$$

By applying the linear interpolation scheme in Eq. (10), the predicted displacement and velocity values for the sub-time step δt can be obtained as

$$\widetilde{\boldsymbol{x}}_{j,n+\frac{s}{m}}^{B_k} = \left(1-\frac{s}{m}\right)\widetilde{\boldsymbol{x}}_{j,n}^{B_k} + \frac{s}{m}\widetilde{\boldsymbol{x}}_{j,n+1}^{B_k}, \quad \widetilde{\dot{\boldsymbol{x}}}_{j,n+\frac{s}{m}}^{B_k} = \left(1-\frac{s}{m}\right)\widetilde{\dot{\boldsymbol{x}}}_{j,n}^{B_k} + \frac{s}{m}\widetilde{\dot{\boldsymbol{x}}}_{j,n+1}^{B_k} \tag{19}$$

Similarly, the EOM of Sub-*k* can be written as s

$$\left(\boldsymbol{A}_k + \boldsymbol{A}_{kj}\right)\ddot{\boldsymbol{x}}_{k,n+1} = \boldsymbol{B}_{k,n+1} + \boldsymbol{D}_{kj,n+1} \tag{20}$$

with

$$\boldsymbol{A}_k = \boldsymbol{M}_k + \gamma_{k,2}\Delta t\boldsymbol{C}_k + \beta_{k,2}\Delta t^2\boldsymbol{K}_k \tag{21}$$

$$\boldsymbol{B}_{k,n+1} = \boldsymbol{F}_{k,n+1} - \boldsymbol{C}_k\widetilde{\dot{\boldsymbol{x}}}_{k,n+1} - \boldsymbol{K}_k\widetilde{\boldsymbol{x}}_{k,n+1} \tag{22}$$

$$\boldsymbol{A}_{kj} = \boldsymbol{M}_j^{B_kB_k} + \gamma_{j,2}\Delta t\boldsymbol{C}_j^{B_kB_k} + \beta_{j,2}\Delta t^2\boldsymbol{K}_j^{B_kB_k} \tag{23}$$

$$\boldsymbol{D}_{kj,n+1} = \begin{bmatrix} -\left(\boldsymbol{c}_j^{B_kB_k}\widetilde{\dot{\boldsymbol{x}}}_{j,n+1}^{B_k} + \boldsymbol{k}_j^{B_kB_k}\widetilde{\boldsymbol{x}}_{j,n+1}^{B_k} + \boldsymbol{c}_j^{B_kB_i}\widetilde{\dot{\boldsymbol{x}}}_{j,n+1}^{B_i} + \boldsymbol{k}_j^{B_kB_i}\widetilde{\boldsymbol{x}}_{j,n+1}^{B_i}\right) \\ \mathbf{0} \end{bmatrix} \tag{24}$$

where $\boldsymbol{M}_j^{B_kB_k} = \begin{bmatrix} \boldsymbol{m}_j^{B_kB_k} & \mathbf{0} \\ \mathbf{0} & \mathbf{0} \end{bmatrix}$, $\boldsymbol{C}_j^{B_kB_k} = \begin{bmatrix} \boldsymbol{c}_j^{B_kB_k} & \mathbf{0} \\ \mathbf{0} & \mathbf{0} \end{bmatrix}$, and $\boldsymbol{K}_j^{B_kB_k} = \begin{bmatrix} \boldsymbol{k}_j^{B_kB_k} & \mathbf{0} \\ \mathbf{0} & \mathbf{0} \end{bmatrix}$

It can be seen from Eqs. (11) and (20), Sub-*j* should provide the terms $\boldsymbol{A}$ and $\boldsymbol{D}$ to Sub-*i* and Sub-*k*, and then Sub-*i* and Sub-*k* solve their EOM and provide the updated acceleration $\ddot{\boldsymbol{x}}$ at the interface boundaries to Sub-*j*. Herein, Sub-*j* is referred to as the primary subsystem, while Sub-*i* and Sub-*k* are referred to as secondary subsystems. The data exchange strategy is shown in Figure 2.

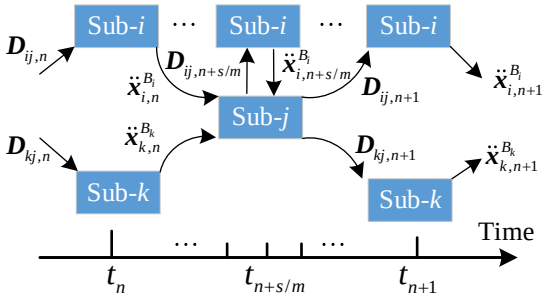

Figure 2. Data exchange strategy

STABILITY ANALYSIS

This section evaluates the numerical stability of the proposed method using the amplification matrix approach. Based on Eqs. (5) and (11), the compact form of EOM for Sub-*i* can be written as

$$\mathbb{K}_i \mathbb{X}_{i,n+(s/m)} = \mathbb{F}_{i,n+(s/m)} - \left(\mathbb{N}_i + \mathbb{D}_{ij}^{B_i}\right) \mathbb{X}_{i,n+(s-1)/m} + \left(1 - \frac{s}{m}\right) \mathbb{D}_{ij}^{B_k} \mathbb{X}_{j,n-1}^{B_k} + \frac{s}{m} \mathbb{D}_{ij}^{B_k} \mathbb{X}_{j,n}^{B_k} \tag{25}$$

where

$$\mathbb{K}_i = \begin{bmatrix} \boldsymbol{A}_i + \boldsymbol{A}_{ij} & \mathbf{0} & \mathbf{0} \\ -\gamma_{i,2}\delta t \mathbf{I} & \mathbf{I} & \mathbf{0} \\ -\beta_{i,2}\delta t^2 \mathbf{I} & \mathbf{0} & \mathbf{I} \end{bmatrix}, \mathbb{X}_{i,n+s} = \begin{bmatrix} \ddot{\boldsymbol{x}}_{i,n+(s/m)} \\ \dot{\boldsymbol{x}}_{i,n+(s/m)} \\ \boldsymbol{x}_{i,n+(s/m)} \end{bmatrix}, \mathbb{F}_{i,n+(s/m)} = \begin{bmatrix} \boldsymbol{F}_{i,n+(s/m)} \\ \mathbf{0} \\ \mathbf{0} \end{bmatrix} \tag{26}$$

$$\mathbb{N}_i = \begin{bmatrix} \gamma_{i,1}\delta t \boldsymbol{C}_i + \beta_{i,1}\delta t^2 \boldsymbol{K}_i & \boldsymbol{C}_i + \delta t \boldsymbol{K}_i & \boldsymbol{K}_i \\ -\gamma_{i,1}\delta t \mathbf{I} & -\mathbf{I} & \mathbf{0} \\ -\beta_{i,1}\delta t^2 \mathbf{I} & -\delta t \mathbf{I} & -\mathbf{I} \end{bmatrix}, \mathbb{D}_{ij}^{B_i} = \begin{bmatrix} \gamma_{j,1}\delta t \boldsymbol{C}_j^{B_iB_i} + \beta_{i,1}\delta t^2 \boldsymbol{K}_j^{B_iB_i} & \boldsymbol{C}_j^{B_iB_i} + \delta t \boldsymbol{K}_j^{B_iB_i} & \boldsymbol{K}_j^{B_iB_i} \\ \mathbf{0} & \mathbf{0} & \mathbf{0} \\ \mathbf{0} & \mathbf{0} & \mathbf{0} \end{bmatrix} \tag{27}$$

$$\mathbb{D}_{ij}^{B_k} = -\begin{bmatrix} \gamma_{j,1}\Delta t \boldsymbol{C}_j^{B_iB_k} + \beta_{j,1}\Delta t^2 \boldsymbol{K}_j^{B_iB_k} & \boldsymbol{C}_j^{B_iB_k} + \Delta t \boldsymbol{K}_j^{B_iB_k} & \boldsymbol{K}_j^{B_iB_k} \\ \mathbf{0} & \mathbf{0} & \mathbf{0} \\ \mathbf{0} & \mathbf{0} & \mathbf{0} \end{bmatrix}, \mathbb{X}_{j,n}^{B_k} = \begin{bmatrix} \ddot{\boldsymbol{x}}_{j,n}^{B_k} \\ \dot{\boldsymbol{x}}_{j,n}^{B_k} \\ \boldsymbol{x}_{j,n}^{B_k} \end{bmatrix} \tag{28}$$

where $\boldsymbol{C}_j^{B_iB_k} = \begin{bmatrix} \mathbf{0} \\ \boldsymbol{c}_j^{B_iB_k} \end{bmatrix}, \boldsymbol{K}_j^{B_iB_k} = \begin{bmatrix} \mathbf{0} \\ \boldsymbol{k}_j^{B_iB_k} \end{bmatrix}$

Subsequently, the set of solutions for small steps *s* from 1 to *m* can be assembled as

$$\begin{bmatrix} \mathbb{K}_i & \mathbf{0} & \dots & \mathbf{0} \\ \mathbb{N}_i + \mathbb{D}_{ij}^{B_i} & \mathbb{K}_i & \ddots & \vdots \\ \vdots & \ddots & \ddots & \mathbf{0} \\ \mathbf{0} & \mathbf{0} & \mathbb{N}_i + \mathbb{D}_{ij}^{B_i} & \mathbb{K}_i \end{bmatrix} \begin{bmatrix} \mathbb{X}_{i,n+\frac{1}{m}} \\ \mathbb{X}_{i,n+\frac{2}{m}} \\ \vdots \\ \mathbb{X}_{i,n+1} \end{bmatrix} = \begin{bmatrix} \mathbb{F}_{i,n+\frac{1}{m}} \\ \mathbb{F}_{i,n+\frac{2}{m}} \\ \vdots \\ \mathbb{F}_{i,n+1} \end{bmatrix} - \begin{bmatrix} \mathbb{N}_i + \mathbb{D}_{ij}^{B_i} \\ \mathbf{0} \\ \vdots \\ \mathbf{0} \end{bmatrix} \mathbb{X}_{i,n} + \begin{bmatrix} \frac{m-1}{m}\mathbf{I} \\ \frac{m-2}{m}\mathbf{I} \\ \vdots \\ \mathbf{0} \end{bmatrix} \mathbb{D}_{ij}^{B_k} \mathbb{X}_{j,n-1}^{B_k} + \begin{bmatrix} \frac{1}{m}\mathbf{I} \\ \frac{2}{m}\mathbf{I} \\ \vdots \\ \mathbf{I} \end{bmatrix} \mathbb{D}_{ij}^{B_k} \mathbb{X}_{j,n}^{B_k} \quad (29)$$

Similarly, based on Eq. (20), the compact form of EOM for Sub-*k* can be written as

$$\mathbb{K}_k \mathbb{X}_{k,n+1} = \mathbb{F}_{k,n+1} - \left(\mathbb{N}_k + \mathbb{D}_{kj}^{B_k}\right) \mathbb{X}_{k,n} + \mathbb{D}_{kj}^{B_i} \mathbb{X}_{j,n+(m-1)/m}^{B_i} \quad (30)$$

where

$$\mathbb{K}_k = \begin{bmatrix} \boldsymbol{A}_k + \boldsymbol{A}_{kj} & \mathbf{0} & \mathbf{0} \\ -\gamma_{k,2}\Delta t\mathbf{I} & \mathbf{I} & \mathbf{0} \\ -\beta_{k,2}\Delta t^2\mathbf{I} & \mathbf{0} & \mathbf{I} \end{bmatrix}, \mathbb{X}_{k,n+1} = \begin{bmatrix} \ddot{\boldsymbol{x}}_{k,n+1} \\ \dot{\boldsymbol{x}}_{k,n+1} \\ \boldsymbol{x}_{k,n+1} \end{bmatrix}, \mathbb{N}_k = \begin{bmatrix} \gamma_{k,1}\Delta t\boldsymbol{C}_k + \beta_{k,1}\Delta t^2\boldsymbol{K}_k & \boldsymbol{C}_k + \Delta t\boldsymbol{K}_k & \boldsymbol{K}_k \\ -\gamma_{k,1}\Delta t\mathbf{I} & -\mathbf{I} & \mathbf{0} \\ -\beta_{k,1}\Delta t^2\mathbf{I} & -\Delta t\mathbf{I} & -\mathbf{I} \end{bmatrix} \quad (31)$$

$$\mathbb{F}_{k,n+1} = \begin{bmatrix} \boldsymbol{F}_{k,n+1} \\ \mathbf{0} \\ \mathbf{0} \end{bmatrix}, \mathbb{D}_{kj}^{B_k} = \begin{bmatrix} \gamma_{j,1}\Delta t\boldsymbol{C}_j^{B_kB_k} + \beta_{k,1}\Delta t^2\boldsymbol{K}_j^{B_kB_k} & \boldsymbol{C}_j^{B_kB_k} + \Delta t\boldsymbol{K}_j^{B_kB_k} & \boldsymbol{K}_j^{B_kB_k} \\ \mathbf{0} & \mathbf{0} & \mathbf{0} \\ \mathbf{0} & \mathbf{0} & \mathbf{0} \end{bmatrix} \quad (32)$$

$$\mathbb{D}_{kj}^{B_i} = -\begin{bmatrix} \gamma_{j,1}\delta t\boldsymbol{C}_j^{B_kB_i} + \beta_{j,1}\delta t^2\boldsymbol{K}_j^{B_kB_i} & \boldsymbol{C}_j^{B_kB_i} + \delta t\boldsymbol{K}_j^{B_kB_i} & \boldsymbol{K}_j^{B_kB_i} \\ \mathbf{0} & \mathbf{0} & \mathbf{0} \\ \mathbf{0} & \mathbf{0} & \mathbf{0} \end{bmatrix}, \mathbb{X}_{j,n+\frac{m-1}{m}}^{B_i} = \begin{bmatrix} \ddot{\boldsymbol{x}}_{j,n+\frac{m-1}{m}}^{B_i} \\ \dot{\boldsymbol{x}}_{j,n+\frac{m-1}{m}}^{B_i} \\ \boldsymbol{x}_{j,n+\frac{m-1}{m}}^{B_i} \end{bmatrix} \quad (33)$$

where $\boldsymbol{C}_j^{B_kB_i} = \begin{bmatrix} \boldsymbol{c}_j^{B_kB_i} \\ \mathbf{0} \end{bmatrix}, \boldsymbol{K}_j^{B_kB_i} = \begin{bmatrix} \boldsymbol{k}_j^{B_kB_i} \\ \mathbf{0} \end{bmatrix}$

Based on the continuity of acceleration assumed at the boundaries and the use of the Nemark-β time integration schemes, the recursive form of Sub-*j* response at the boundaries B_i and B_k can be compactly expressed as

$$\mathbb{X}_{j,n+(m-1)/m}^{B_i} = \mathbb{T}_{ji}\mathbb{X}_{i,n+(m-1)/m} \text{ and } \mathbb{X}_{j,n+1}^{B_k} = \mathbb{T}_{jk}\mathbb{X}_{k,n+1} \quad (34)$$

with

$$\mathbb{T}_{ji} = \begin{bmatrix} \mathbf{0} & \mathbf{I} & \mathbf{0} & \mathbf{0} & \mathbf{0} & \mathbf{0} \\ \mathbf{0} & \mathbf{0} & \mathbf{0} & \mathbf{I} & \mathbf{0} & \mathbf{0} \\ \mathbf{0} & \left(\beta_{j,2} - \beta_{i,2}\right)\delta t^2\mathbf{I} & \mathbf{0} & \mathbf{0} & \mathbf{0} & \mathbf{I} \end{bmatrix} \text{ and } \mathbb{T}_{jk} = \begin{bmatrix} \mathbf{I} & \mathbf{0} & \mathbf{0} & \mathbf{0} & \mathbf{0} & \mathbf{0} \\ \mathbf{0} & \mathbf{0} & \mathbf{I} & \mathbf{0} & \mathbf{0} & \mathbf{0} \\ \left(\beta_{j,2} - \beta_{k,2}\right)\Delta t^2\mathbf{I} & \mathbf{0} & \mathbf{0} & \mathbf{0} & \mathbf{I} & \mathbf{0} \end{bmatrix} \quad (35)$$

After combining Eqs. (29), (30) and (34), the solution of the entire system can be written as

$$\mathbb{X}_{n+1} = \mathbb{A}\mathbb{X}_n \quad (36)$$

where $\mathbb{X}_n = \begin{bmatrix} \mathbb{X}_{i,n} & \mathbb{X}_{j,n-\frac{1}{m}}^{B_i} & \mathbb{X}_{j,n-1}^{B_k} & \mathbb{X}_{j,n}^{B_k} & \mathbb{X}_{k,n} \end{bmatrix}^T$; $\mathbb{A}$ is the amplification matrix of the proposed method which can be written as

$$\mathbb{A} = \begin{bmatrix} \mathbb{A}_{11} & \mathbb{A}_{12} & \mathbb{A}_{13} \\ \mathbb{A}_{21} & \mathbb{A}_{22} & \mathbb{A}_{23} \\ \mathbb{A}_{31} & \mathbb{A}_{32} & \mathbb{A}_{33} \end{bmatrix} \tag{37}$$

where

$$\mathbb{A}_{11} = \boldsymbol{\Psi}^m,\ \mathbb{A}_{12} = \begin{bmatrix} \mathbf{0} & \sum_{s=1}^{m}\left(1-\frac{s}{m}\right)\boldsymbol{\Psi}^{m-s}\mathbb{K}_i^{-1}\mathbb{D}_{ij}^{B_k} & \sum_{s=1}^{m}\frac{s}{m}\boldsymbol{\Psi}^{m-s}\mathbb{K}_i^{-1}\mathbb{D}_{ij}^{B_k} \end{bmatrix},\ \mathbb{A}_{13} = \mathbf{0} \tag{38}$$

$$\mathbb{A}_{21} = \begin{bmatrix} \mathbb{T}_{ji}\boldsymbol{\Psi}^{m-1} \\ \mathbf{0} \\ \mathbb{T}_{jk}\mathbb{K}_k^{-1}\mathbb{D}_{kj}^{B_i}\mathbb{T}_{ji}\boldsymbol{\Psi}^{m-1} \end{bmatrix},\ \mathbb{A}_{23} = \begin{bmatrix} \mathbf{0} \\ \mathbf{0} \\ -\mathbb{T}_{jk}\mathbb{K}_k^{-1}\left(\mathbb{N}_k + \mathbb{D}_{kj}^{B_k}\right) \end{bmatrix} \tag{39}$$

$$\mathbb{A}_{22} = \begin{bmatrix} \mathbf{0} & \mathbb{T}_{ji}\sum_{s=1}^{m}\left(1-\frac{s}{m}\right)\boldsymbol{\Psi}^{m-s-1}\mathbb{K}_i^{-1}\mathbb{D}_{ij}^{B_k} & \mathbb{T}_{ji}\sum_{s=1}^{m}\frac{s}{m}\boldsymbol{\Psi}^{m-s-1}\mathbb{K}_i^{-1}\mathbb{D}_{ij}^{B_k} \\ \mathbf{0} & \mathbf{0} & \mathbf{I} \\ \mathbf{0} & \mathbb{T}_{jk}\mathbb{K}_k^{-1}\mathbb{D}_{kj}^{B_i}\mathbb{T}_{ji}\sum_{s=1}^{m}\left(1-\frac{s}{m}\right)\boldsymbol{\Psi}^{m-s-1}\mathbb{K}_i^{-1}\mathbb{D}_{ij}^{B_k} & \mathbb{T}_{jk}\mathbb{K}_k^{-1}\mathbb{D}_{kj}^{B_i}\mathbb{T}_{ji}\sum_{s=1}^{m}\frac{s}{m}\boldsymbol{\Psi}^{m-s-1}\mathbb{K}_i^{-1}\mathbb{D}_{ij}^{B_k} \end{bmatrix} \tag{40}$$

$$\mathbb{A}_{31} = \mathbb{K}_k^{-1}\mathbb{D}_{kj}^{B_i}\mathbb{T}_{ji}\boldsymbol{\Psi}^{m-1},\ \ \mathbb{A}_{33} = -\mathbb{K}_k^{-1}\left(\mathbb{N}_k + \mathbb{D}_{kj}^{B_k}\right) \tag{41}$$

$$\mathbb{A}_{32} = \begin{bmatrix} \mathbf{0} & \mathbb{K}_k^{-1}\mathbb{D}_{kj}^{B_i}\mathbb{T}_{ji}\sum_{s=1}^{m}\left(1-\frac{s}{m}\right)\boldsymbol{\Psi}^{m-s-1}\mathbb{K}_i^{-1}\mathbb{D}_{ij}^{B_k} & \mathbb{K}_k^{-1}\mathbb{D}_{kj}^{B_i}\mathbb{T}_{ji}\sum_{s=1}^{m}\frac{s}{m}\boldsymbol{\Psi}^{m-s-1}\mathbb{K}_i^{-1}\mathbb{D}_{ij}^{B_k} \end{bmatrix} \tag{42}$$

with $\boldsymbol{\Psi} = -\mathbb{K}_i^{-1}\left(\mathbb{N}_i + \mathbb{D}_{ij}^{B_i}\right)$.

k_i

To determine the numerical stability limit of the proposed method, it is necessary to find the maximum time step beyond which the spectral radius of $\mathbb{A}$ is greater than one. The spectral radius refers to the largest eigenvalue of the amplification matrix $\mathbb{A}$.

For different combinations of the implicit Newmark-β integration scheme (Newmark average acceleration method, NAA) and the explicit Newmark-β integration scheme (Explicit Newmark method, ENM) for Sub-*i* and Sub-*k* of the four-DOFs system. The time step to ensure stability can be maximized if the integration coefficients of Sub-*j* can satisfy the requirements as given in Table 1. More details about these requirements can be found in Reference (Wang et al. 2024).

Table 1 Numerical stability requirements

	Integration scheme	
Sub-*i*	Sub-*j*	Sub-*k*
NAA	$\gamma_{j,1} = \gamma_{j,2} = 1/2$, $\beta_{j,1} = 1/2 - \beta_{j,2}$, and $\beta_{j,2} = 1/2$	NAA
ENM	$\gamma_{j,1} = \gamma_{j,2} = 1/2$, $\beta_{j,1} = 1/2 - \beta_{j,2}$, and $\beta_{j,2} = \max\left(\frac{1}{4\lambda^{B_i}} + \frac{1}{2}, \frac{1}{4\lambda^{B_k}} + \frac{1}{2}\right)$	ENM
ENM	$\gamma_{j,1} = \gamma_{j,2} = 1/2$, $\beta_{j,1} = 1/2 - \beta_{j,2}$, and $\beta_{j,2} = \frac{1}{4\lambda^{B_i}} + \frac{1}{2}$	NAA

Note: $\lambda^{B_i} = k_j/k_i$ and $\lambda^{B_k} = k_j/k_k$

For cases with NAA used for all secondary subsystems, the proposed method maintains unconditional stability regardless of the time step ratio; For cases with ENM used for secondary subsystems, the proposed method is conditionally stable as well, and the stability can be improved with the increase of the time step ratio *m*.

APPLICATION OF THE NUCLEAR STRUCTURE

To demonstrate the potential of the proposed method for SSI analysis of nuclear structures, a Candu 6 containment structure (Radulescu et al. 1997) is considered, as shown in Figure 3. The nuclear structure has dimensions of 45.3 m (width) × 54.2 m (height). Given the system's symmetry and assuming seismic input occurs only along the global X-axis, half of the structure with the soil domain was modeled. The structure was assumed to be linear elastic (density = 2,400 kg/m³, elastic modulus = 32.3 GPa, Poisson's ratio = 0.15) and simulated with C3D10 in ABAQUS. In addition, the structure was assumed to be placed on the surface of a generic soil domain representing standard plant design conditions (Korea Electric Power Corporation and Korea Hydro & Nuclear Power Co. 2013). The soil domain measures 200 m (length) × 100 m (width) × 112.8 m (depth) and exhibits shear wave velocities ranging from 300 m/s for upper layers to 1,000 m/s for deeper layers. The soil was modeled with C3D8 elements in ABAQUS.

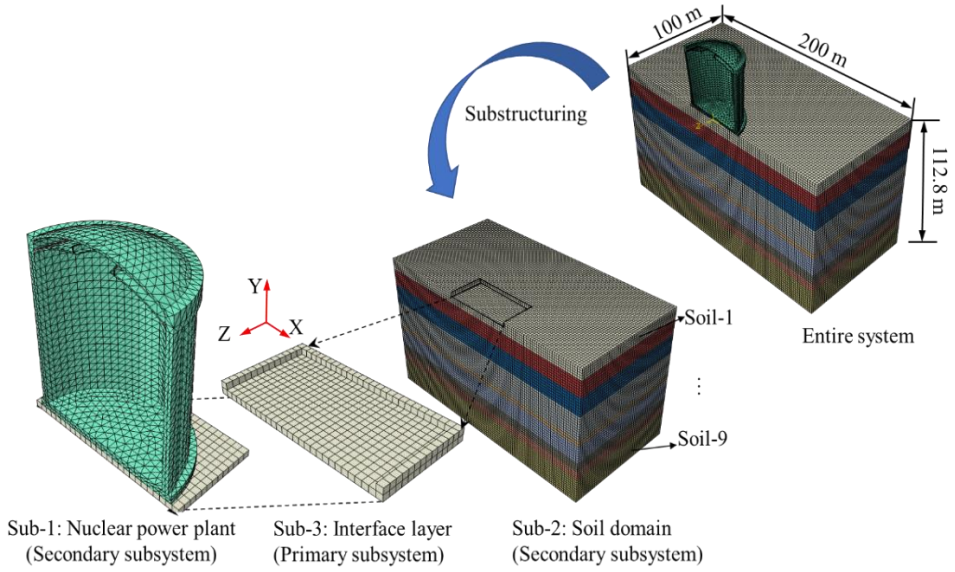

Figure 3. The entire SSI system and the decomposed subsystems

Based on the proposed method, the SSI system was decomposed into three subsystems as shown in Figure 3. The details of them are as follows:

- Sub-1: this secondary subsystem includes the nuclear containment building and the surface layer of the soil elements that were assumed to be perfectly tied with the bottom foundation surface. The EOM of it was solved through the NAA integration scheme with a time step of 0.001 s.

- Sub-2: this secondary subsystem includes the majority of the soil domain. The NAA integration scheme was used with a time step of 0.004 s.

- Sub-3: this primary subsystem includes a single layer of the soil elements between the two secondary subsystems in the above, and the integration coefficients are $\gamma_{j,1} = \gamma_{j,2} = 1/2$, $\beta_{j,1} = 1/2 - \beta_{j,2}$, and $\beta_{j,2} = 1/2$

For comparison with the integrated model, a standalone model simulates the SSI system using a time step of 0.001 s. Figure 4 compares the displacement magnitude contours at 2.948 s for both models, while Figure 5 shows the relative displacement time histories at various locations of the containment building. The good agreement between the integrated and standalone models verifies the accuracy of the proposed method. Regarding computational efficiency, both models were executed on the same desktop computer (Intel® Xeon® Gold 6226R CPU @ 2.90GHz, 64.0 GB RAM). The standalone model required 37.27 hours, whereas the integrated model (employing time steps of 0.001 s (Sub1) and 0.004 s (Sub2)) completed in 26.30 hours, representing a 29.43% reduction in computational time. Such improvement demonstrates the advantage of using different time steps.

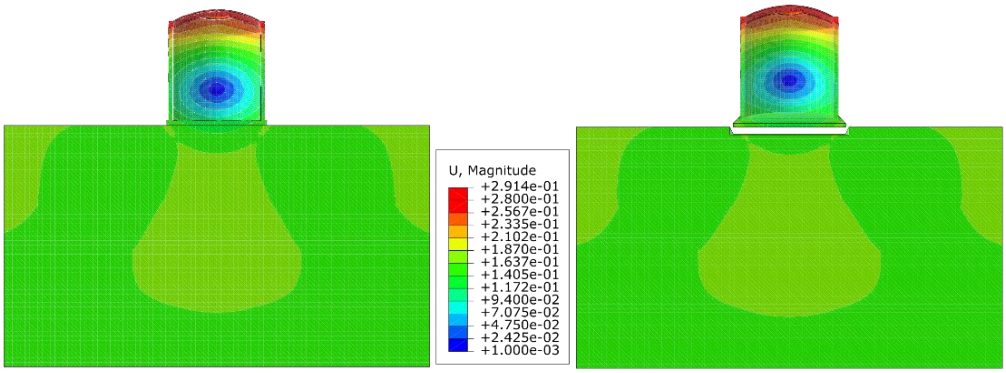

Fig. 4. Displacement amplitude contour plot at 2.948s: (a) standalone model (b) integrated model.

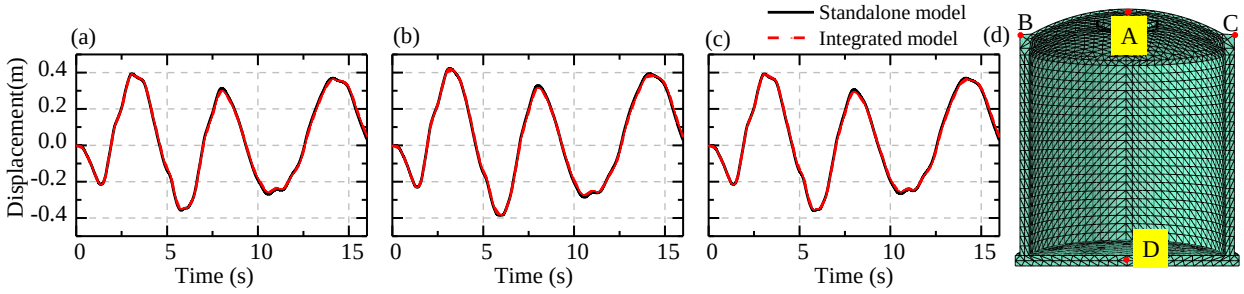

Fig. 5. Displacement time histories of containment building relative to node D: (a) Point A; (b) Point B; (c) Point C.

CONCLUSION

This study presents the extension of the WHK integrated simulation method for different time steps analysis. Similar to the WHK method, the method can be easily implemented in existing finite element software. The numerical stability can be systematically evaluated through the amplification matrix method and unconditionally stable solutions can be achieved regardless of the time-step ratio. The accuracy and numerical stability of the method are verified through its application to SSI analysis of a nuclear containment structure. By comparing with the standalone model, the integrated model using the proposed different-step approach maintains good accuracy and improves computational efficiency.

REFERENCES

Chen, S., Lv, H., and Zhou, G. (2022). "Partitioned Analysis of Soil-Structure Interaction for Nuclear Island Buildings." *Earthquake Engineering & Structural Dynamics*, 51 (10): 2220-2247.

Gregory B Bunting (2016). Parallel Real-Time Hybrid Simulation of structures using multi-scale models. *Purdue University*.

Huang, X. and Kwon, O.-S. (2020). "An integrated simulation method for coupled dynamic systems". Computer-Aided Civil and Infrastructure Engineering, 35(10), 1115-1131.

Huang, X., Kwon, O.-S., and Moon, I. (2024). "Integrated Nonlinear Soil-Structure Interaction Analysis of a Nuclear Contain for Beyond Design-Basis Earthquake." *Transactions of the SMiRT 27*. Yokohama.

Korea Electric Power Corporation, and Korea Hydro & Nuclear Power Co. L. (2013). "*Seismic Design Bases for the APR1400 Standard Plant Design*". Rochville, Maryland, United States.

Radulescu, J. P., Pradolin, L., and Mamet, J. C., (1997). "Ultimate Pressure Capacity of CANDU 6 Containment Structures." CNS proceedings of the 1997 CNA/CNS annual conference on powering Canada's future. Montreal.

Wang, S., Huang, X., Kwon, O.-S., Wu, B., and Yang, G. (2024). "Numerically Stable Integrated Simulation Method for Coupled Dynamic Systems." *Journal of Structural Engineering*, 150 (12): 04024182.